Theor Chem Account (2008) 119:177–190
DOI 10.1007/s00214-007-0390-7

REGULAR ARTICLE

A configurational and conformational study of aframodial and its diasteriomers via experimental and theoretical VA and VCD spectroscopies

K. J. Jalkanen · Julian D. Gale · P. R. Lassen · L. Hemmingsen · A. Rodarte · I. M. Degtyarenko · R. M. Nieminen · S. Brøgger Christensen · M. Knapp-Mohammady · S. Suhai

Received: 21 April 2007 / Accepted: 6 September 2007 / Published online: 25 October 2007

Abstract In this work we present the experimental and theoretical vibrational absorption (VA) and the theoretical vibrational circular dichroism (VCD) spectra for aframodial. In addition, we present the theoretical VA and VCD spectra for the diasteriomers of aframodial. Aframodial has four chiral centers and hence has $2^4 = 16$ diasteriomers, which occur in eight pairs of enantiomers. In addition to the four chiral centers, there is an additional chirality due to the helicity of the entire molecule, which we show by presenting 12 configurations of the 5S,8S,9R,10S enantiomer of aframodial. The VCD spectra for the diasteriomers and the 12 configurations of one enantiomer are shown to be very sensitive not only to the local stereochemistry at each chiral center, but in addition, to the helicity of the entire molecule. Here one must be careful in analyzing the signs of the VCD bands due to the 'non-chiral' chromophores in the molecule, since one has two contributions; one due to the inherent chirality at the four chiral centers, and one due to the chirality of the side chain groups in specific conformers, that is, its helicity. Theoretical simulations for various levels of theory are compared to the experimental VA recorded to date. The VCD spectra simulations are presented, but no experimental VCD and Raman spectra have been reported to date, though some preliminary VCD measurements have been made in Stephens' lab in Los

Festschrift in Honor of Philip J. Stephens' 65th Birthday.

K. J. Jalkanen (✉) · J. D. Gale
Nanochemistry Research Institute, Department of Applied Chemistry, Curtin University of Technology, P.O. Box U1987, Perth 6845, Western Australia
e-mail: jalkanen@ivec.org
URL: http://www.nanochemistry.curtin.edu.au/people/staff/karl.cfm

P. R. Lassen
Department of Physics, Technical University of Denmark, 2800 Kgs. Lyngby, Denmark

L. Hemmingsen
University of Copenhagen, Thorvaldsenvej 40, 1871 Frederiksberg C, Denmark
e-mail: lhe@life.ku.dk

A. Rodarte
Hartnell College, Administrative Information Systems C113, 156 Homestead Avenue, Salinas, CA 93901, USA
e-mail: arodarte@hartnell.edu

I. M. Degtyarenko · R. M. Nieminen
Laboratory of Physics, Helsinki University of Technology, P.O.B. 1100, 02015 Hut, Finland
e-mail: imd@fyslab.hut.fi

R. M. Nieminen
e-mail: rni@fyslab.hut.fi

S. Brøgger Christensen
Department of Medicinal Chemistry, Faculty of Pharmaceutical Sciences, Copenhagen University, Universitetsparken 2, 2100 Copenhagen Ø, Denmark
e-mail: sbc@farma.ku.dk

M. Knapp-Mohammady · S. Suhai
Department of Molecular Biophysics, German Cancer Research Center (Deutsches Krebsforschungszentrum), 69120 Heidelberg, Germany
e-mail: m.knapp@dkfz-heidelberg.de

S. Suhai
e-mail: s.suhai@dkfz.de

P. R. Lassen
Selandia-CEU, Willemoesvej 4, 4200 Slagelse, Denmark
e-mail: prla@selandia-ceu.dk

Angeles. The flexible side chain is proposed to be responsible for the small size of the VCD spectra of this molecule, even though the chiral part of the molecule is very rigid and has four chiral centers. In addition to VCD and Raman measurements, Raman optical activity (ROA) measurements would be very enlightening, as in many cases bands which are weak in both the VA and VCD, may be large in the Raman and/or ROA spectra. The feasibility of using vibrational spectroscopy to monitor biological structure, function and activity is a worthy goal, but this work shows that a careful theoretical analysis is also required, if one is to fully utilize and understand the experimental results. The reliability, reproduceability and uniqueness of the vibrational spectroscopic experiments and the information which can be gained from them is discussed, as well as the details of the computation of VA, VCD and Raman (and ROA) spectroscopy for molecules of the complexity of aframodial, which have multiple chiral centers and flexible side chains.

Keywords Conformational analysis · Vibrational spectroscopy · VA · VCD · DFT · PBE · B3LYP · Aframodial

1 Introduction

Aframodial, (+)-(E)-8β(17)-epoxylabd-12-ene-15,16 dial, has been isolated from seeds of *Aframomum danielli* [1]. Its chemical abstracts index name is 2-[2-[(1R,2S,4aS, 8aS)-octahydro-5,5,8a)-trimethylspiro[napthalene-2(1H),2′-oxiran]-1-yl]ethylidene]-,(2E)-butanedial, Fig. 1. It has also been isolated from the seeds and rhizomes of *Afamomum alboviolaceum* (Ridley) Schum (Zingiberaceae) [2]. It has subsequently been found to have both antifungal and antileukemic activity [3], in addition to antiplasmodial activity [4]. Aframodial has also been shown to have an inhibitory effect against cholesterol biosynthesis and has been assumed to be a hydroxymethylglutaryl-coenzyme A (HMG-CoA) reductase inhibitor [5]. This molecule has four chiral centers in a tricyclic ring system with a dial side chain. The conformational flexibility of the side chain and the absolute configuration at the four chiral centers are the focus of this experimental and theoretical study. Here we combine a conformational and configurational study utilizing density functional theory (DFT) at the B3LYP/6-31G* level to first determine the structures of the eight diasteriomers of aframodial. In addition to the study of the diasteriomers, we will study the conformational energy space for the dial side chain. Here by comparing the measured vibrational circular dichroism (VCD) spectra of the enantiomer synthesized or found in nature with the one calculated it is possible to determine the absolute configuration, since the signs of the VCD peaks either (in theory) all agree or are the opposite.

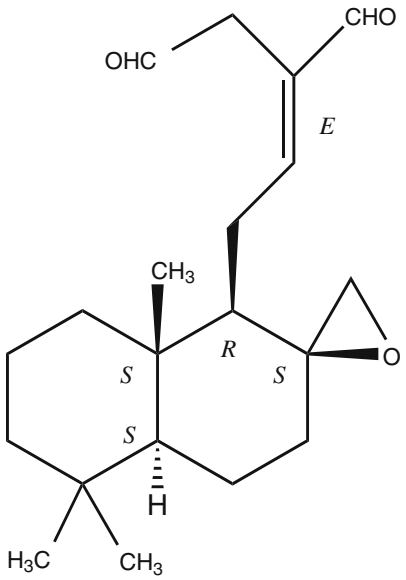

(+)-Aframodial

2-[2-[(1R,2S,4aS,8aS)-octahydro-5,5,8a-trimethylspiro[naphthalene-2(1H),2'-oxiran]-1-yl]ethylidene]-, (2E)-butanedial

CAS reg No: 71641-23-1

Fig. 1 (+)Aframoidal: (+)2-[2-[(1R,2S,4aS,8aS)-octahydro-5,5,8a)-trimethylspiro[napthalene-2(1H),2′-oxiran]-1-yl]ethylidene]-,(2E)-butanedial

Previously VCD has been used to determine the absolute configuration of molecules with only one chiral center. The situation changes entirely when one has four chiral centers, as here one must be able to assign the VCD features due to the individual chiral centers. In many cases the modes may be localized to one chiral center, but in others, the modes may comprise motions involving more than one chiral center. Hence the analysis of the VCD spectra is no longer straightforward. Here one can look upon this as a weakness of VCD, but we see it as a strength, since it yields more information (in theory), although once again the analysis is more involved. The absolute configuration (chirality) of the substituted decaline, a related molecule, has been determined [6,7].

Previously vibrational absorption (VA), VCD, Raman and Raman optical activity (ROA) spectroscopic methods have been used to answer structural questions in a variety of biological molecules, L-alanine (LA) [8–12], *N*-acetyl L-alanyl N′-methylamide (NALANMA) [8,12–16], L-alanyl L-alanine (LALA) [8,17,18], 3-methyl indole [19], tri-L-serine [20], phenyloxirane [21], and Leu-enkephalin [22]. Here the influence of the environment was shown to be very important. This was in part due to the inherent flexibility in these molecules, which is present in aframodial's side chain, but not the decalin system which contains the four chiral centers. In the case of the LA and LALA, the species

in the isolated state, NH_2CHCH_3COOH and $NH_2CHCH_3CONHCHCH_3COOH$, are not the same as that found in an aqueous environment, $NH_3^+CHCH_3COO^-$ and $NH_3^+CHCH_3CONHCHCH_3COO^-$ (the so-called zwitterionic states). To stabilize the zwitterionic state required us to treat the aqueous environment. Initially we added a small number of waters [8]. Subsequently, we increased the number of water molecules and also embedded the LA and LALA + N water molecule complexes within spherical cavities and treated these systems with the Onsager continuum model [9,11,17,18]. The best of these structures was then used as the geometry at which we calculated the Hessian, the atomic polar tensors (APT), the atomic axial tensors (AAT), the electric dipole-electric dipole polarizability derivatives (EDEDPD), the electric dipole-magnetic dipole polarizability derivatives (EDMDPD), and the electric dipole-electric quadrupole polarizability derivatives (EDEQPD), which allowed us to simulate the VA, the VCD, the Raman and the ROA spectra of LALA and its deuterated isotopomers [9,11,18].

For the case of NALANMA the species does not change when one goes from the isolated state or that in a nonpolar solvent to an aqueous solvent, but the vibrational spectra were very different. Here the original thought was that one could either use continuum models to treat the effect due to the aqueous environment or to totally neglect the solvent and compare calculations performed on the isolated state of the molecule with measurements made in the aqueous environment [14]. Our modeling study showed that four of the water molecules in the first solvation shell were required and actually part of the stable structure in aqueous solution [15]. This structure was later confirmed by NMR studies, where one previously has not been able to be explained due to only including the solute [23,24].

In the case of 3-methyl indole we were able to perform calculations on the isolated state of the molecule and compare to measurements made in nonpolar solvents. Here we found very good agreement between our predicted Raman scattering spectra and that measured. We also presented the Raman scattering spectra for the neutral radical and the radical cation, both thought to be important possible intermediates in many biological mechanisms. These calculations provide the experimentalists the predicted frequencies and intensities which can then be compared to the parent species. This helps in identifying which regions in the VA, VCD and Raman spectra to look for these species. In many cases the bands due to the species of interest are buried under those of the noninteresting species. Here the theoretical predictions can add a lot to the experimental studies. By not having to treat the solvent either implicitly or explicitly, this of course makes the modeling much easier and should also be performed as a first step in understanding the inherent properties of the molecule under investigation. Other groups have utilized the QM/MM model to calculate some molecular properties, for example, the electric dipole and quadrupole moments [25]. Others have compared the methods on how to do the MD, that is, whether it is better to use the Car-Parrinello or the Born-Oppenheimer approaches [26]. In addition to new methods to simulate biomolecules in aqueous solution, recently advanced spectroscopic techniques have been developed to probe the vibrational relaxation pathways in water [27]. Here one can further test the theoretical methods to see if they are consistent and able to reproduce these experimental results. In addition, empirical corrections have been made to *ab initio* and DFT methods to correct for their deficiencies which result in systematic errors, which these empirical corrections try to account for [28,29].

On the experimental side, vibrational spectroscopy has been extended in the range of applications, both the possible mediums being measured and the size of the samples, extending from the single molecule all the way to macroscopic proportions, that is, cells and aggregates of cells forming tissues. Here one is interested in understanding not only the properties of individual molecules, but also the properties of the macroscopic entities; how and even if one can gain information about the mechanisms and understanding of molecular complexes by studying individual molecules. The hope is that we can not only gain understanding from the studies of individual molecules, but also gain understanding of the synergistic relationships between the individual molecules and the new properties and physical properties that arise from the aggregate or combined whole. In these systems, the truth is that the properties and function of the whole is not a simple sum of the properties and functions of the individual parts. Here we must also understand and find the new properties and principles which arise. The simplest case of this was found in our study of *N*-acetyl L-alanine *N*′-methylamide and four water molecules. The structure of NALANMA found in the aqueous environment is not a stable stucture without the aqueous environment present. Hence even though we think that studies of individual molecules are important to understand the inherent isolated state properties of the molecules, we do not want to underemphasize the multitude of new features which are only possible through the synergistic nature of interactions, first simple two body, and three body interactions, and finally many *N* body interactions, which are responsible for the new stuctures and new functions. Just like the function of a motor being distinct from the function of its many individual parts, so are biological functions of molecular complexes and aggregates distinct from the functions of the individual molecules.

At an even higher level the N and M body objects further interact (self assemble) to create new entities, with unique properties and features which are due to the synergistic and cooperative interactions with the system(s). The idea is that the simple laws and models of physics, chemistry and biology

developed to date for modeling and understanding individual atoms and molecules will not in general be applicable to many complex systems and phenomena. By using this paradigm we will actually be adding unnecessary complexity. But to create new simpler models, we must be able to generate new functionals and be able to indentify which properties (variables) change and are responsible for changes in biological function.

New forms of vibrational spectroscopy have been and are being developed with the hope that they can contribute to the problem of determining the structures of biomolecules, biomolecular complexes and even aggregate structures in aqueous solution and other biological environments [30–32]. Vibrational spectroscopy adds the possibility to see the contributions from individual molecules and even individual parts within molecules, that is, the many conformers, structures, complexes and/or aggregates which exist on the time scale of the experiment, in contrast to the picture gained from the NMR and X-ray and neutron diffraction experiments, which in many cases gives an average picture of the structure, complex or aggregate. Knowledge of how the structures and dynamics of the individual parts are changed by new and changing environments is fundamental to gain an in depth understanding of how biochemical nanomachines work.

In studying aframodial we look at another type of important biological molecule, a tricyclic molecule which has four chiral centers. Due to the four chiral centers there is the possibility to have the same connectivity but different absolute configurations of the functional groups in space, so called diasteriomers. Aframodial is a derivative of labdane. Labdanes as well as the enantiomeric series entlabdanes are naturally occurring. Even though both of the two enantiomers of (+)-(E)-labd-12,8(17)-diene-15,16-dial, an analogue of aframodial, in which the exocyclic epoxy group has been deoxygenated to a double bond, have not been obtained from the same plant, the two isomers have been isolated from closely related species, the (+)-isomer from *Alpinia galanga* [33] and from *Aframomum sceptrum* [4] and the (−)-isomer from *Alpinia speciosa* [34]. In the case of aframodial only the (+)-isomer has been reported even though it has been isolated from a broad spectrum of species belonging to the Zingiberaceae including *Alpinia galanga* [35], *Alpinia katsumadai* [36], *Aframomum daniellii* [37], and *Aframomum latifolium* [4].

Aframodial [(+)-(E)-8β(17)-epoxylabd-12-ene-15,16-dial] (absolute configuration: 5S,8S,9R,10S) was originally isolated from *Aframomum danielli* (Hook f.) [1]. Later studies have revealed the presence of this compound in *A. polyanthum*, *A. masuianum*, *A. kayserianum* [38], and in smaller amounts in *Alpinia galanga*, *Zingiber officinalis* [38], *Aframomum sulcatum* [4], *A. alboviolaceum* [2], and *A. latifolium* [4]. All of these plants belong to the family Zingiberaceae. The hot taste of *A. danielli* was correlated to the presence of aframodial [1] and later studies have shown a number of biological *in vitro* effects including modest cytotoxicity [39], modest antifungal properties [39] and modest antiplasmodial activities [4]. In vivo mice experiments have revealed that aframodial is a poorly toxic antihypercholesterolemic agent. The structural similarities between aframodial and mevastatin have led to the suggestion that the two compounds both reduce cholesterol level by inhibiting hydroxymethylglutaminate coenzyme A reductase (HMG-CoA reductase) [5]. The relative and absolute configuration of aframodial was established by correlation to sclareol [1]. The absolute configuration of sclareol has been elucidated [6]. The absolute configuration of (+)-(E)-labd-12,8(17)-diene-15,16-dial, in which the epoxy group is reduced to an exocyclic methylene group, has been determined by application of the octant rule on the cyclohexanone obtained after ozonolysis [39]. Since the two closely related compounds the epoxide and the exocyclic methylene have been isolated from the same plant they most likely possess the same stereochemistry at the stereogenic centres. Both studies reveal that the decaline moiety of aframodial and mevastatin possess the same stereochemistry at comparable stereogenic centres. The decaline moieties of mevastatin and aframodial both have a limited number of possible conformations. In contrast the side chains are very flexible. The present study has enabled characterisation of a preferred conformation of the side chains in aframodial.

The bicyclic labdane system with correct stereochemistry might be formed by protonation of the 14,15-double bond of E,E,E-geranylgeranylpyrophoshate provoking a cascade reaction, which eventually affords the carbon skeleton if the geranylgeranylpyrophosphate adopt one of the two favorable conformations. The stereochemical outcome is defined by the preferred conformation: the one conformation will afford the (+)-series, whereas the other conformation will afford the (−)-series [40]. Since the two conformations are mirror images of each other both are equal likely and consequently a racemic mixture is expected if no enzyme directs the stereochemistry of the reaction. If the cyclization takes place on the surface of an enzyme, however, this enzyme will define the stereochemical outcome. Consequently the presence of both enantiomers indicates the absence of a directing enzyme, whereas a stereoselective formation of only one enantiomer suggest the presence of a directing enzyme. In the case of aframodial different cyclases must direct the cyclization in *Alpinia galanga* [33] and in *Alpinia speciosa* [34].

The format of the presentation is as follows. In the methods and materials section we discuss the isolation of aframodial from nature and how the experimental VA measurements were made. Additionally the methods and methodology we used to investigate the potential energy surface of the 5S,8S, 9R,10S (SSRS will be used to shorten the notation) enantiomer of aframodial and also the various diasteriomers, to

determine the relative energies of the diasteriomers and the conformers of the SSRS enantiomer, and finally to simulate the VA and VCD spectra of the various diasteriomers and conformers. In the results and discussion section we compare the energies of the various diasteriomers and the various conformers of the SSRS enantiomer. In this section we also present the simulated VA and VCD spectra for all diasteriomers and conformers of the SSRS enantiomer and compare the experimentally measured VA spectrum to our simulations for the SSRS enantiomer. Finally in the conclusion section we give the conclusions we have arrived at from this combined theoretical and experimental study of aframodial.

2 Methods and materials section

2.1 Experimental: extraction of aframodial from seeds of *Aframomum danielli*, purification and preparation of solutions for VA and VCD measurements

Isolation

Aframodial was isolated from *Aframomum latifolium* as previously described [4]. Briefly dried fruits were extracted with ethyl acetate, the extract filtered and the filtrate concentrated in vacuo. The residue was suspended in water–ethyl acetate (1:1) and the ethyl acetate phase concentrated. The residue was chromatographed over silica gel using toluene to which increasing amounts of ethyl acetate were added as an eluent. Further chromatography over Lichroprep RP18 using water–methanol (7:2) to which increasing amounts of water were added afforded aframodial as colourless crystals.

A solution which was used for the IR/VA measurements was prepared as follows: 6 mg of aframodial (powder form) was dissolved in 300 ml of chloroform (Aldrich). The VA and VCD spectra were measured on a Thermo Nicolet Nexus 870 FTIR spectrometer (at Thermo Fischer in Madison, WI, USA) equipped with a photoelastic molelator (PEM) module, a mercury cadmium telluride (MCT) detector and a potasium bromide (KBr) cell with a 50 μm spacer.

2.2 Theoretical simulations

With the GaussView builder from Gaussian Inc. we built the SSRS enantiomer of aframodial [41]. Starting from this structure we performed a geometry optimization at the B3LYP/6-31G* level of theory. After we had the B3LYP/6-31G* optimized structure for this one diasteriomer, we inverted the stereochemistry at the four chiral centers and then we also inverted at pairs of centers to generate seven more starting geometries, for which we also performed B3LYP/6-31G* geometry optimizations. At the B3LYP/6-31G* optimized structures we subsequently calculated the Hessians, APT and the AAT, which allowed us to simulate the VA and VCD spectra for the eight diasteriomers. After observing that the VCD signal for the two C=O carbonyl stretch frequencies were positive for all eight diasteriomers we performed geometry optimizations for the various side chain conformers of the SSRS enantiomer of aframodial. Here we found 12 local minima and at each local minimum we performed Hessians, APT and AAT calculations which allowed us to simulate the VA and VCD spectra.

In addition to investigating the conformational space of the two C=O relative to one another, we also optimized the geometries for the trans isomer (about the C=C bond) for the six lowest energy conformers, by rotating about the C=C bond in the six optimized structures calculated at the B3LYP/6-31G* level. This saves some time in the optimization, since the geometrical parameters used in the model builder are not optimal for the ring structure. This can save a lot of CPU time.

In addition to investing these conformational energy spaces (that is, finding the local energy minimum with respect to these degrees of freedom), we have also rotated about the C11–C12 and C9–C11 bonds of the side chain to see if we had found the lowest energy structure with respect to these torsional angles. The C11–C12 bond involves a rotation about a bond between sp2 and sp3 centers, similar to those involving the two aldehyde groups. The C11–C12 and C9–C11 bond are defined in the results section.

3 Results and Discussion

3.1 Energetics and structural changes in various diasteriomers of aframodial at the B3LYP/6-31G* level of theory

In Figs. 2, 3 and 4, we present the optimized structures for aframodial (5S,8S,9R,10S or SSRS) and its seven diasteriomers: four epimers (5S,8R,9R,10S; 5S,8S,9S,10S; 5S,8S,9R,10R; and 5R,8S,9R,10S) and the three diepimers (5S,8R,9S,10S; 5S,8R,9R,10R; and 5R,8R,9R,10S). See figure captions for the details.

In Table 1 one can see the relative energies for the structure of aframodial (SSRS) and its seven diasteriomers (four epimers and three diepimers) we have found to date along with the eight torsion angles which define the chirality at the four chiral centers. Note that inversion at the chiral centers of the two fused rings also causes distortions (or changes) in the configurations of the ring as shown in Table 2. In the SSRS configuration the two rings are both in boat configurations. The angles of the boat configuration of the two six membered rings are (starting from the dimethyl ring carbon) −27.25, −29.95, 62.95, −38.88, −14.35, 49.30 (ideal angles: −30, −30, 60, −30, −30, 60); 70.63, −30.73, −30.97, 57.96,

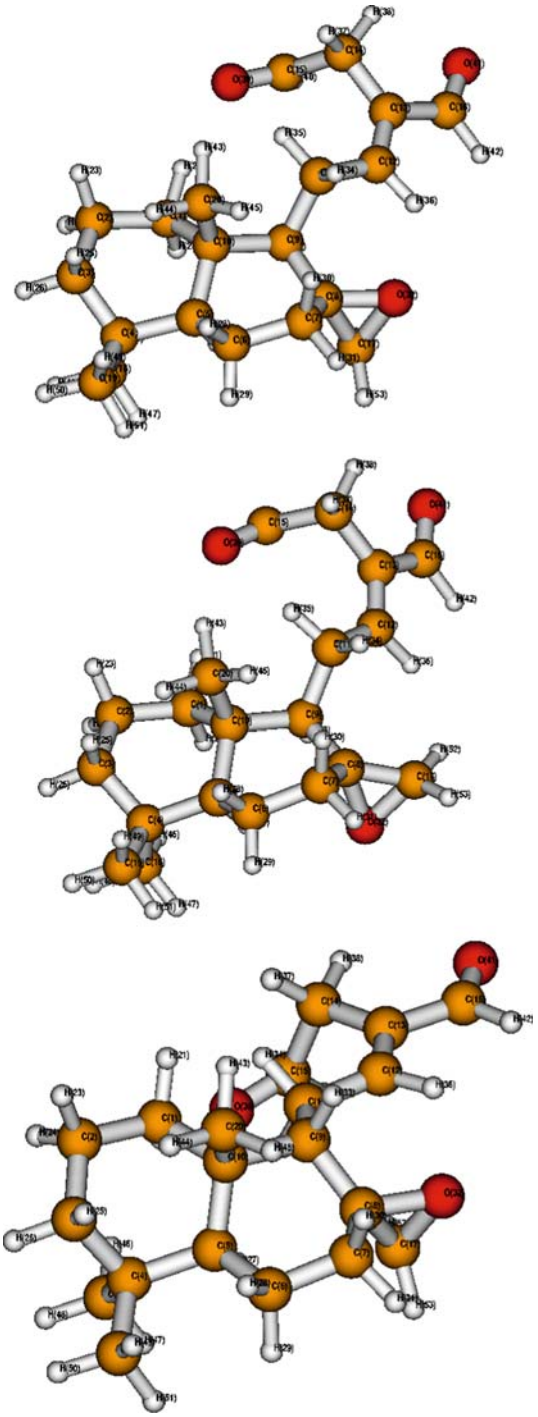

Fig. 2 Aframodial 5S,8S,9R,10S (*top*) and two disasteriomers (*epimers*) 5S,8R,9R,10S and 5S,8S,9S,10S (*middle and bottom*)

−17.13, −44.92 (60, −30, −30, 60, −30, −30), respectively. These angles do not change much in the SRRS and SSSS diasteriomers as seen in Table 2. Hence the rings maintain their configurations when the inversion is at either the carbon in the second ring (C_9) with the side chain or at the carbon containing the oxirane ring (C_8).

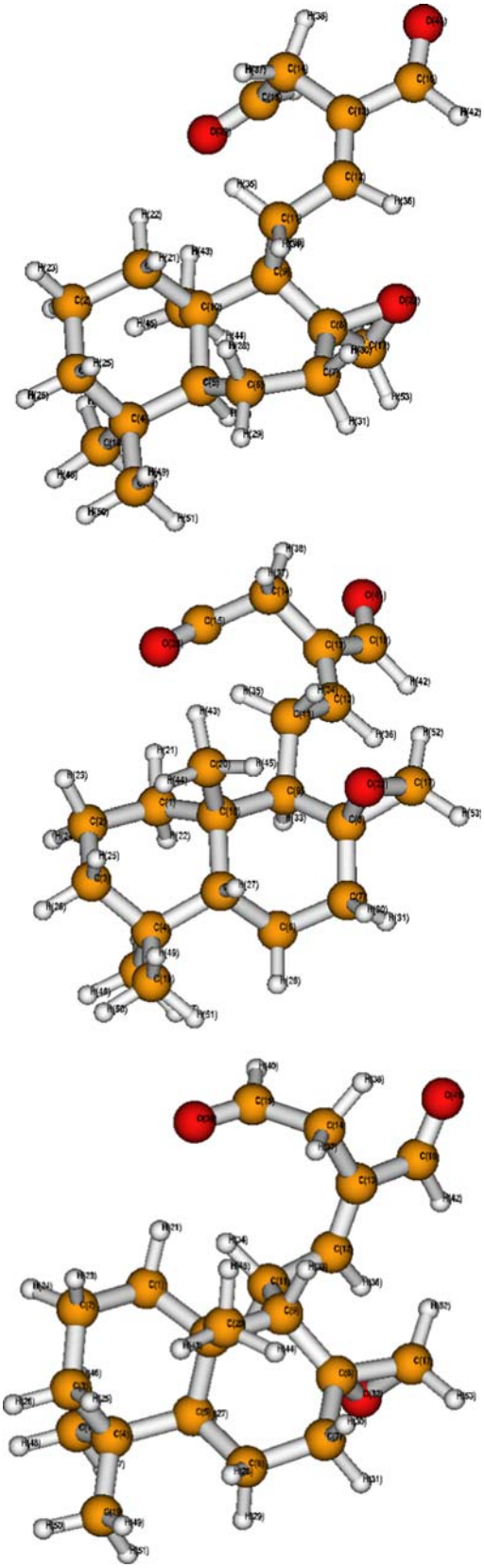

Fig. 3 Aframodial diasteriomers (epimers) 5S,8S,9R,10R and 5R, 8S,9R,10S (*top* and *middle*), diasteriomer (diepimer) 5S,8R,9S,10R (*bottom*)

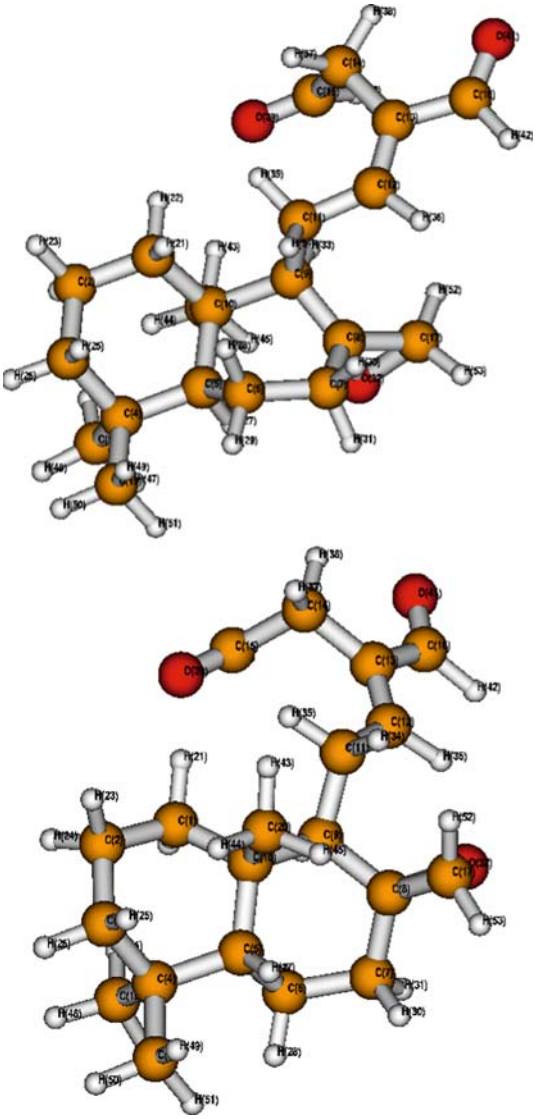

Fig. 4 Aframodial diasteriomers (diepimers) 5S,8R,9R,10R and 5R, 8R,9R,10S (*top* and *bottom* correspondingly)

In the SSRR diasteriomer (where there is an inversion at one of the bridging carbons, in this case the one at the top of the two adjoining rings (C10)) one can see from Table 2 that the first ring has changed from its boat configuration to the chair configuration (ideal angles: −60, 60, −60, 60, −60, 60). The second ring has changed to the inverted boat configuration (ideal angles: 30, 30, −60, 30, 30, −60).

In the RSRS diasteriomer the first ring again has the boat configuration which is actually closer to ideal than that in the SSRS, SRRS and SSSS diasteriomers. The second ring also has the boat configuration, though the angles are not ideal, hence the boat has some distortion.

In the SRSS diasteriomer the two rings have the same two boat configurations as in the SSRS, SRRS, SSSS and RSRS diasteriomers.

In the SRRR diasteriomer the first ring has again converted to the chair configuration as it has in the SSRR diasteriomer. Here we have inversion at two of the carbons, the top bridging carbon (C10) and the ring carbon of the oxirane ring (C8). The second ring now has an inverted boat configuration as it had in the SSRR diasteriomer.

In the RRRS diasteriomer the first ring is again in the boat configuration as is the second ring. Hence only the diasteriomers with inversion at the top carbon of the fused ring (C10) cause the rings to change their configurations, that is, the first ring converts from the boat to the chair and the second ring converts from a boat to an inverted boat configuration. Since nature has made aframodial by enzymatic means in the plant, the diasteriomer produced does not necessarily need to be the lowest energy diasteriomer. Indeed, the SSRS diasteriomer thought to be that found in nature is not. At least in our work here, it is found to be 4.14 kcal/mole higher in energy than the RRRS diasteriomer. Also the RSRS, SSRR and the SRRR diasteriomers are lower in energy, being 0.67, 0.74 and 1.11 kcal/mole higher in energy than the SSRS diasteriomer, respectively. Note that this may change when the side chain configuration is modified. All of the diasteriomer calculations were made with the same side chain configuration with respect to the fused ring systems. Another possibility to determine the relative energies of only the fused ring systems would be to replace the side chain by either a methyl group or only a hydrogen. Indeed we have performed the earlier to see which modes in the SSRS diasteriomer were due to only the side chain and also to investigate the coupling between the modes of the fused ring system and the side chain. This will be discussed in the next subsection.

3.2 Changes in the VA and VCD spectra in diasteriomers of aframodial

In Fig. 5 we present the VA spectra for the aframodial and its seven diasteriomers. In Fig. 6 we present the VCD spectra for the aframodial and its seven diasteriomers. As one can see in the fingerprint region of the IR/VA spectra the diasteriomers are different. Enantiomers have the identical IR/VA spectra and mirror image VCD spectra, but diasteriomers have different spectra. Since the conformation of the side chain was the same for aframodial and its seven diasteriomers, the C=O stretch regions are very similar. The fingerprint region in the IR/VA spectra can be used to distinguish which diasteriomer is present, and the VCD spectra can be used to identify which enantiomer for each set of diasteriomers.

In addition to the changes observed in VA and VCD spectra for aframodial and its seven diasteriomers, we have also investigated changes in the backbone angles of the side chain, especially the relative orientation of the two aldehyde groups for aframodial, one enantiomer of one of the eight sets of diasteriomers. This is because we wanted to see how sen-

Table 1 Relative energies in kcal/mole of aframodial and 7 diasteriomers calculated at the B3LYP/6-31G* level of theory

Diasteriomer	B3LYP/6-31G*	$C_1C_{10}C_5C_6$	$C_1C_{10}C_5H_{27}$	$C_{10}C_9C_8O_{32}$	$C_{10}C_9C_8C_{17}$	$C_1C_{10}C_9C_{11}$	$C_1C_{10}C_9H_{33}$	$C_2C_1C_{10}C_5$	$C_2C_1C_{10}C_{20}$
SSRS	4.14	−172.84¶	74.92	−169.93†	122.34	85.48∗	−31.11	62.95‡	−60.05
SRRS	6.80	−172.57	75.32	103.92	170.94†	84.07	−34.19	62.96	−60.19
SSSS	7.89	−168.12	79.60	−169.67	121.86	−17.52	99.41∗	61.69	−61.67
SSRR	0.74	−85.48	160.64	159.69	92.08	18.32	−98.48	−51.61	71.09‡
RSRS	0.67	102.85	−142.48¶	−74.70	−142.72	70.49	−46.82	59.08	−60.99
SRSS	7.43	−165.74	81.70	120.10	−172.22†	−30.46	86.30∗	63.13	−60.80
SRRR	1.11	−85.51	160.73	71.57	138.50†	18.93	−98.23	−51.61	71.40‡
RRRS	0.00	102.95	−142.27¶	−159.37	−90.43†	68.27	−48.07	58.79	−61.42

Absolute energy for RRRS = −1005.789295 Hartrees. ¶, †, * and ‡ demarcate the change of a chiral center

Table 2 Ring torsion angles for aframodial and 7 diasteriomers calculated at the B3LYP/6-31G* level of theory

Diasteriomer	$\tau_{4,3,2,1}$	$\tau_{3,2,1,10}$	$\tau_{2,1,10,5}$	$\tau_{1,10,5,4}$	$\tau_{10,5,4,3}$	$\tau_{5,4,3,2}$	$\tau_{6,5,10,9}$	$\tau_{5,10,9,8}$	$\tau_{10,9,8,7}$	$\tau_{9,8,7,6}$	$\tau_{8,7,6,5}$	$\tau_{7,6,5,10}$
SSRS	−27.25	−29.95	62.95	−38.88	−14.35	49.30	70.63	−30.73	−30.97	57.96	−17.13	−44.92
SRRS	−27.55	−29.66	62.96	−38.93	−14.49	49.61	71.02	−31.34	−30.43	57.58	−17.02	−45.18
SSSS	−27.74	−30.75	61.69	−34.76	−19.77	52.82	69.48	−27.70	−34.17	59.65	−16.57	−45.55
SSRR	−58.09	59.21	−51.61	44.12	−43.89	50.40	37.67	22.82	−62.74	34.30	30.50	−67.79
RSRS	−27.80	−32.07	59.08	−26.52	−29.09	58.31	−16.32	−41.58	61.13	−16.99	−43.02	60.90
SRSS	−25.55	−33.60	63.13	−33.31	−22.03	53.38	71.93	−37.44	−18.96	46.71	−12.21	−45.16
SRRR	−58.24	59.26	−51.61	44.00	−43.76	50.47	37.65	23.01	−63.34	35.08	29.70	−67.42
RRRS	−28.15	−31.75	58.79	−26.37	−29.23	58.53	−16.60	−42.55	64.62	−20.75	−40.72	60.86

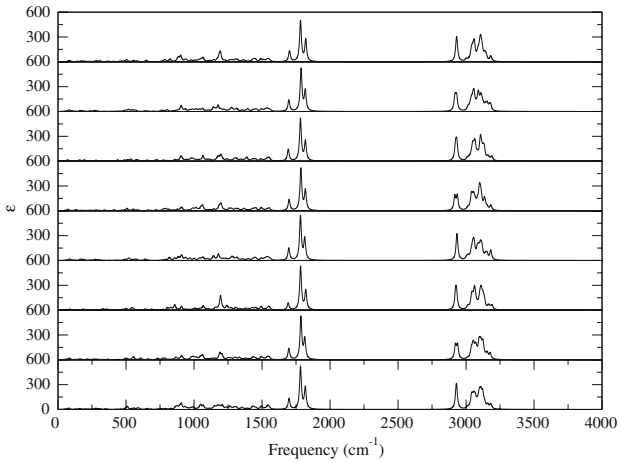

Fig. 5 VA spectra for aframodial and 7 diasteriomers

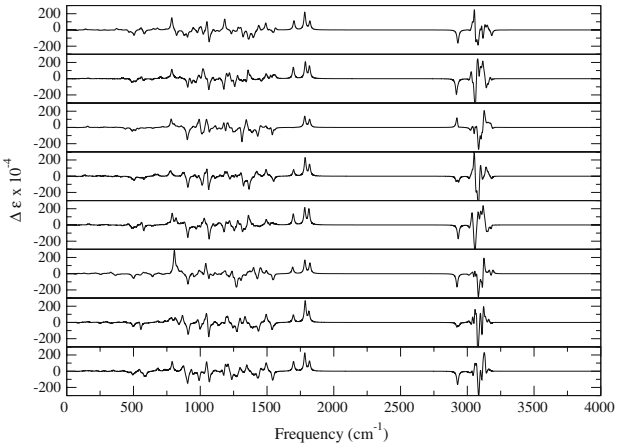

Fig. 6 VCD spectra for aframodial and 7 diasteriomers

sitive the VA and VCD spectra were with respect to these changes. This investigation was motivated by the fact that the VCD signals of all eight diasteriomers calculated all had two positive bands (due to the same conformation for the side chains). Hence the inversion at the four chiral centers did not seem to have a large effect on the VCD of the two C=O stretch modes of the two aldehyde groups as can be seen in Fig. 6, where we present the VCD spectra for aframodial and its seven diasteriomers.

3.3 Couping between the modes observed in the VA and VCD spectra in the side chain of the SSRS diasteriomer and the fused ring system

To be able to investigate which modes are due to the side chain of the SSRS enantiomer of aframodial, one replaces the side chain by a methyl group. This preserves the chiral centers but removes the modes due to the side chain. It also allows us to see how significant the coupling is between the

Table 3 Relative energies (kcal/mole) of the different conformers of SSRS enantiomer of aframodial calculated at the B3LYP/6-31G* level of theory

Enantiomer	B3LYP/6-31G*	$\tau_{O_{39}C_{15}C_{14}C_{13}}$	$\tau_{C_{15}C_{14}C_{13}C_{16}}$	$\tau_{C_{14}C_{13}C_{16}O_{41}}$	$\tau_{C_{14}C_{13}C_{12}C_{11}}$	$\tau_{C_{13}C_{12}C_{11}C_9}$	$\tau_{C_{12}C_{11}C_9C_{10}}$
g+g+t	−1005.77565523(4.42)	114.50	103.61	−177.15	0.71	132.99	−154.07
g+g+c	−1005.78269471(0.00)	112.45	100.89	−0.92	0.15	131.00	−156.68
g-g-c	−1005.78265893(0.02)	−113.68	−105.43	0.58	−0.05	90.07	−159.08
g-g-t	−1005.77558433(4.46)	−115.74	−106.92	178.75	−0.20	91.54	−157.73
g+g-t	−1005.77344356(5.81)	122.94	−86.37	−178.23	2.86	118.28	−152.19
g+g-c	−1005.77880465(2.44)	157.98	−53.48	3.51	−0.01	105.79	−155.81
g-g+c	−1005.77891533(2.37)	−159.46	55.30	−3.72	0.56	116.47	−155.32
g-g+t	−1005.77349463(5.77)	−120.62	81.82	−178.90	−0.60	117.19	−153.15
c-g-c	−1005.78055296(1.34)	−13.01	−110.13	−1.54	1.51	113.92	−155.44
c-g-t	−1005.77364902(5.68)	−13.32	−109.57	−177.00	1.74	127.26	−153.51
c+g+t	−1005.77518822(4.71)	11.03	94.52	179.44	−0.14	99.51	−158.24
c+g+c	−1005.78249229(0.13)	13.29	95.13	1.42	−0.12	98.63	−159.15

modes of the coupled ring system and the side chain. As this compound is not found in nature, it could either be synthesized in the lab, or one could attempt to replace the side chain chemically with a methyl group to perserve the chirality at this chiral centre.

3.4 Understanding of aframodial conformations: side chain structural elements

In order to understand how the two carbonyl stretch frequencies are affected by their relative orientations, we have calculated the relative energies of 12 conformers which differ by the values of the three torsional angles which define their relative orientation in the side chain. The relative energies (kcal/mole) and the values of the torsional angles are given in Table 3. As one can see the g+g+c conformer is lowest in energy. This is the conformer which we used in the diasteriomer calculations. This calculated VCD intensity for the two aldehydic carbonyl stretch frequencies (modes) is consistent with the observed VCD intensity. Hence the predicted VCD signal of the bands from the lowest energy conformer for this part of the side chain is consistent with the bands observed in the experimental VCD spectrum. In Figs. 7 and 8 we present the VA and VCD spectra for the 12 conformers of the aframodial (SRRS). From the VCD spectra in Fig. 8 one can see that only for conformers 1 (g+g+c) and 6 (g-g+c) with positive VCD signals for the C=C and two C=O stretch modes do we have agreement with the positive features in our preliminary experimental VCD spectrum (not presented due to small signal to noise). We are having the VCD spectrum remeasured in the laboratory of Prof. P.J. Stephens at the University of Southern California, in Los Angeles, where one of us, KJJ, received his PhD. As one can see in Fig. 7 the C=O stretch region dominated the IR/VA spectrum in the mid IR region. The absorbance in this region was optimal for the VCD measurement, but if one recalls, the two carbonyl groups are present in the flexible side chain. Hence

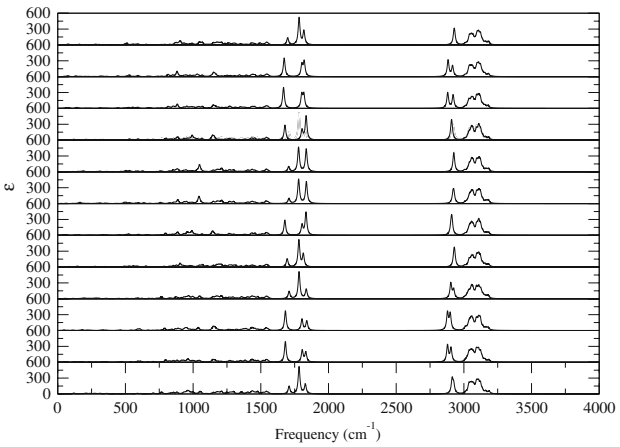

Fig. 7 VA spectra for 12 conformers of SSRS enantiomer of aframodial

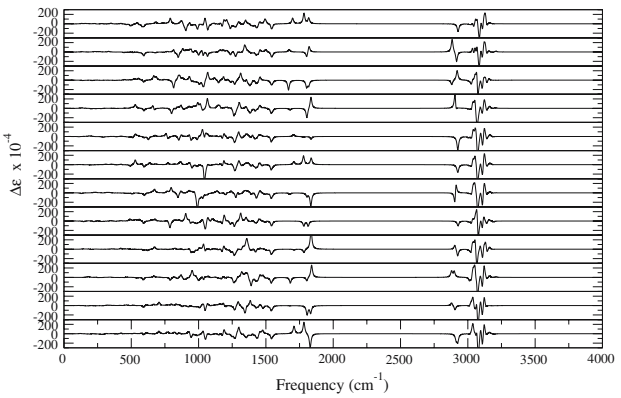

Fig. 8 VCD spectra for 12 conformers of SSRS enantiomer of aframodial

Table 4 Relative energies (kcal/mole) of the different conformers of SSRS enantiomer of aframodial calculated at the B3LYP/6-31G* level of theory with cis and trans at the double bond

Enantiomer	B3LYP/6-31G*	$\tau_{O_{39}C_{15}C_{14}C_{13}}$	$\tau_{C_{15}C_{14}C_{13}C_{16}}$	$\tau_{C_{14}C_{13}C_{16}O_{41}}$	$\tau_{C_{14}C_{13}C_{12}C_{11}}$	$\tau_{C_{13}C_{12}C_{11}C_9}$	$\tau_{C_{12}C_{11}C_9C_8}$
g+g+c(c)	−1005.78269471(0.00)	112.45	100.89	−0.92	0.15	131.00	−156.68
g+g+c(t)	−1005.77603989(4.18)	124.12	77.48	−1.33	179.29	108.96	−156.06
g-g-c(c)	−1005.78265893(0.02)	−113.68	−105.43	0.58	−0.05	90.07	−159.08
g-g-c(t)	−1005.77655367(3.85)	−118.07	−78.78	1.91	−177.46	111.15	−154.58
g+g-c(c)	−1005.77880465(2.44)	157.98	−53.48	3.51	−0.01	105.79	−155.81
g+g-c(t)	−1005.77532006(4.63)	158.84	−58.32	4.93	179.93	110.67	−155.91
g-g+c(c)	−1005.77891533(2.37)	−159.46	55.30	−3.72	0.56	116.47	−155.32
g-g+c(t)	−1005.77532490(4.62)	−157.69	57.83	−5.13	179.87	118.15	−154.46
c-g-c(c)	−1005.78055296(1.34)	−13.01	−110.13	−1.54	1.51	113.92	−155.44
c-g-c(t)	−1005.77789926(3.01)	−9.71	−107.14	−1.45	−172.53	102.20	−154.58
c+g+c(c)	−1005.78249229(0.13)	13.29	95.13	1.42	−0.12	98.63	−159.15
c+g+c(t)	−1005.77594422(4.24)	9.33	73.75	4.16	178.84	108.00	−156.36

if there are many conformers present at room temperature in chloroform solution, with VCD signals which are of opposite sign, then the net VCD signal in this region should be small. This is consistent with our relative energy calculations for the various side chain conformers.

In addition to the conformers due to the three torsional angles for the two aldehyde groups, we have a cis-trans isomerization about the C=C bond. In Table 4 we see that for the six lowest energy structures the trans isomer is always lower in energy than the corresponding cis isomer. For the g+g+c conformer the energy difference is 4.18 kcal/mole between the cis and trans species. For the g-g-c, g+g-c, g-g+c, c-g-c and c+g+c the energy differences are 3.83, 2.19, 2.25, 1.67, and 4.11 kcal/mole, respectively. In all cases the cis species is lower in energy.

In the g+g+c conformer with the cis double bond, the coupling between the lower frequency C=O stretch mode the C=C stretch mode is very low. Also the two C=O modes are closer to the same intensity in the VA spectra. In the VCD spectra these two bands both have a positive VCD. In addition the C=C mode also has a positive VCD signal. Hence the sign pattern VCD signals of these three bands does not change for the cis-trans change. The frequency of the C=C mode is reduced from 1,699 to 1,693 cm^{-1}, a reduction by 6 cm^{-1}, which should be resolvable in the VA and VCD spectra. Since both bands are predicted to have positive VCD signals, the VCD does not help in this case to resolve the two features. Also the energy difference of 4.2 kcal/mole would make the population of the species such that it would probably not be seen in the VA or VCD spectra. But at least the 6 cm^{-1} separation from the trans mode, would make it resolvable if it was present at a high enough level. In Figs. 9 and 10 we present the VA and VCD spectra for the six lowest energy trans conformers. For four of the six conformers the two aldehydic hydrogen stretch frequencies are clearly resolvable in the VA

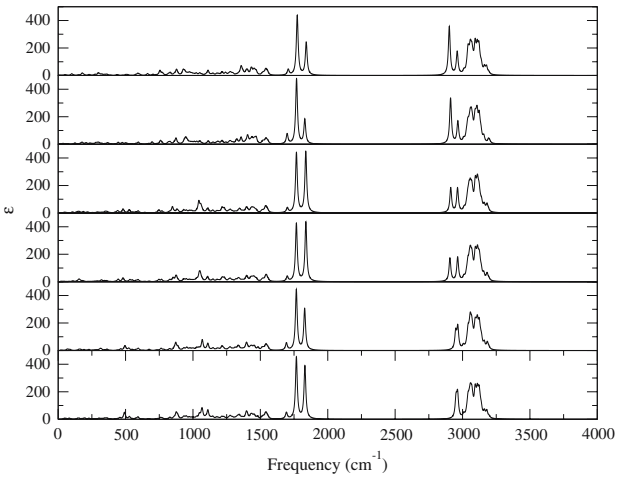

Fig. 9 VA spectra for six lowest energy trans aframodial conformers in Table 4

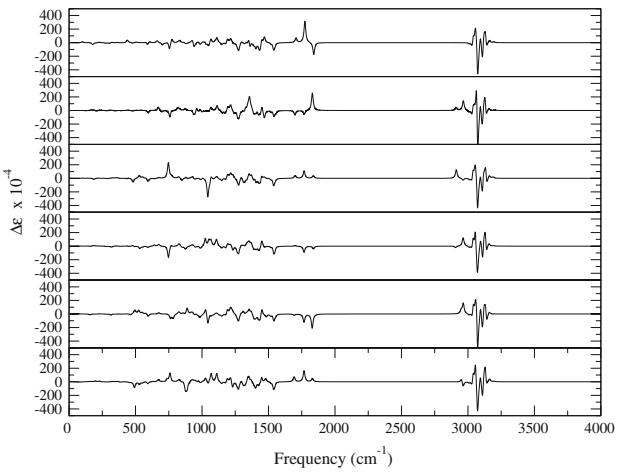

Fig. 10 VCD spectra for six lowest energy trans aframodial conformers in Table 4

Table 5 Relative energies (kcal/mole) of the different side chain conformers of SSRS enantiomer of aframodial calculated at the B3LYP/6-31G* level of theory

Enantiomer	B3LYP/6-31G*	$\tau_{O_{39}C_{15}C_{14}C_{13}}$	$\tau_{C_{15}C_{14}C_{13}C_{16}}$	$\tau_{C_{14}C_{13}C_{16}O_{41}}$	$\tau_{C_{14}C_{13}C_{12}C_{11}}$	$\tau_{C_{13}C_{12}C_{11}C_9}$	$\tau_{C_{12}C_{11}C_9C_{10}}$
g+g+c	−1005.78269471(0.00)	112.45	100.89	−0.92	0.15	131.00	−156.68
g+g+c	−1005.78127582(0.89)	109.09	105.49	−2.11	4.03	−125.48	−150.60
g+g+c	−1005.78269704(0.00)	112.95	102.04	−0.80	0.07	130.94	−157.05
g+g+c	−1005.78056437(1.34)	109.59	72.86	−0.95	−3.80	140.28	−77.52
g+g+c	−1005.77732147(3.37)	124.22	110.26	0.20	−1.04	133.30	87.58

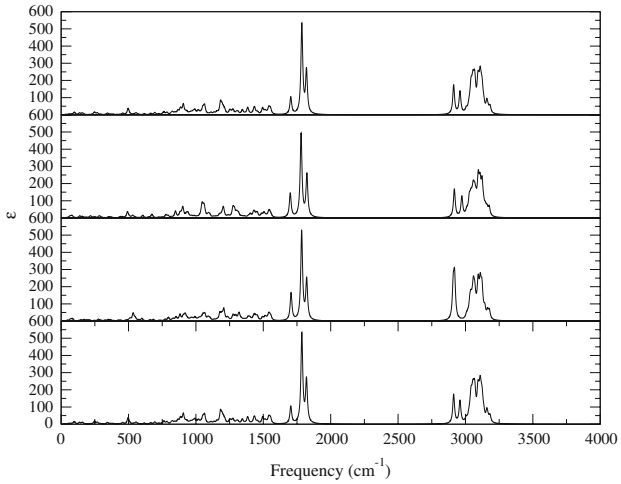

Fig. 11 VA spectra for four unique aframodial conformers in Table 5

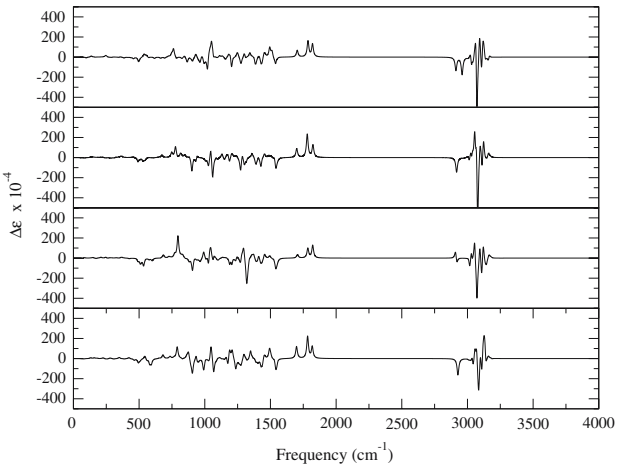

Fig. 12 VCD spectra for four unique aframodial conformers in Table 5

spectra. For the conformers where there is an anisotropy in the aldehydic stretch modes there is also an anisotropy in the two aldehydic C=O stretch modes. In the VCD spectra one can see much larger distinguishing features than in the VA spectra.

In addition to the already discussed torsion angles, we have two additional torsion angles, about the C9–C11 and C11–C12 bonds, respectively. In Table 5 we see that the conformer from Table 3 for the g+g+c conformer is lowest in energy. One other conformer was found by rotating about the C11–C12 bond with an energy higher by 0.89. Starting with an angle of 180° the geometry converged to the structure with this angle being 131. With the value of this angle being 0 degrees there was a steric clash with the atoms of the oxirane ring. The two conformers found by rotating about the C9–C11 bond are 1.34 and 3.37 kcal/mole higher in energy, respectively. In Figs. 11 and 12 we present the IR/VA and VCD spectra for these 4 conformers.

The relative ordering of the energies could of course change for 1 of the 12 other conformers for the aldehyde groups and also for the cis isomer, and we have not done a complete systematic search yet. In a future publication we shall present the complete set of energies. Note also that many of the possible conformers will not actually occur due to steric interactions, as we have already seen with the presented torsional angle variations. In the next section we compare the experimental VA spectra with our aforementioned VA spectral simulations.

3.5 Comparion of theoretical and experimental VA spectra

In Fig. 13 we present the experimental IR/VA spectrum for aframodial in a chloroform solution. Our attempts to measure a publishable VCD spectrum failed so far due to limited amount of sample. Even though the FTIR method gives the complete IR/VCD spectra, for VCD measurements the problem is not so straightforward. This is due to the modulator only being set to quarter wave at one wavelength. In the old dispersive instruments, the modulator was ramped so that it would quarter wave at each wavelength at which the VCD signal was being measured [42]. Using current FTIR VCD instrumentation, there is much more processing of the signal. For a good review of the current state of the art see the works of Nafie et al. at Syracuse University and Rina Dukor of Biotools, Eric Jiang at Thermo Fischer, and Hans Hermann Drews at Bruker Optik. The three main vendors of VCD instrumentation are Biotools-Bomen, Thermo Fischer and Bruker Optik. Each vendor's instrument has its strengths,

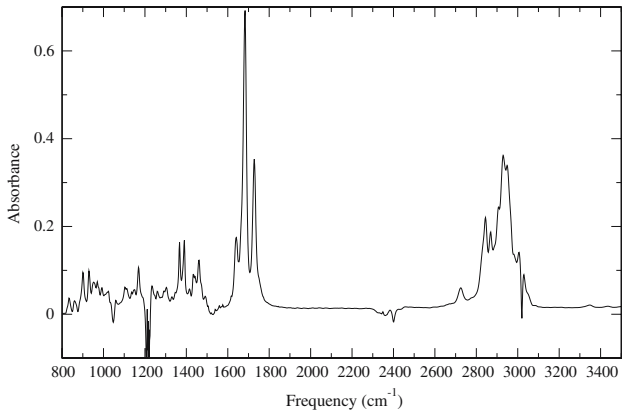

Fig. 13 Experimental VA spectrum for aframodial in $CHCl_3$ solution

and the choice really depends on one's application and level of expertise. VCD is not yet a routine experiment, but gradually it is getting straightforward, especially for samples in non polar organic solvents. VCD of biomolecules in aqueous solution is more challenging, both experimentally and theoretically.

But by comparing the measured IR/VA spectra with those for the many conformers for which we calculated, one can see that there are only a few conformers whose spectra are consistent with the experimental spectrum. Hence even though we have not been able to indentify which conformer (or set of conformers) are present, we can eliminate some. With the VCD spectra and additional Raman and ROA spectra, the conformation of the aframodial side chain should be able to identified. How the spectra change with temperature and solvent polarity would also be important if we are to be able to understand the biological function and activity of aframodial. How it is broken down in the body is also important, since if one wishes to use a derivative of it in the pharmaceutical industry, then we need to solve this problem. And to solve a problem, it is best to completely understand its properties. The combination of experimental VA, VCD, Raman and ROA spectral measurements under a variety of conditions with high level *ab initio* or DFT calcuations, appears to be very promising.

3.6 Alternatives to full DFT calculations: energetics and structural changes in various diasteriomers of aframodial at the SCC-DFTB and SCC-DFTB+D levels of theory

The SCC-DFTB and the dispersion corrected alternative, SCC-DFTB+D, is a density funtional theory based tight binding method. It is based on DFT but is much faster and has been shown to give better accuracy than the previously used semi-empirical wave function based methods, like AM1 and PM3, of similar accuracy to the recently developed semi-empirical methods of Stewart and Thiel. While these methods do good for geometry optimizations and even possibly Hessians/vibrational frequency calculations, it is not obvious that these minimal basis set methods will be able to treat static and dynamic electric and magnetic field perturbations. We have previously showed that the SCC-DFTB method reproduced well the vibrational frequencies and eigenvectors for the alanine dipeptide, *N*-acetyl L-alanine *N*′-methylamide. We combined the SCC-DFTB force field with APTs and AATs from full B3LYP calculations with split valence plus polarized basis sets. This appears to be the minimal size basis set for VA, VCD, Raman and ROA spectral simulations. For quantitative accuracy, the aug-cc-pVTZ and larger basis sets are used [21,43]. Hence what may be the alternative is to use the SCC-DFTB and SCC-DFTB+D for geometry optimizations, Hessian calculations and even molecular dynamic simulations, but to use full DFT and/or first principles ab initio type methods for the tensors, APT, AAT, EDEDPD, EDMDPD and EDEQPD, which are required for the VA, VCD, Raman and ROA intensities. Another alternative is to have separate models for the energy, and hence structural/potential energy profile, and a second model to represent the various molecular property surfaces. This is in the same spirit of Prof. N.C. Handy's group at Cambridge and the CADPAC program: Cambridge Analytical Derivatives Package, where the group has pioneered the work on molecular property derivatives [44]. The first analytical implementation of the AAT was indeed in CADPAC [45], while one of the first analytic implementations of the APT (length formalism) was also in CADPAC [46] and later in the momentum formalism [47,48]. The first analytical implementation of the EDEDPD, required for Raman spectral intensities [49], all with the so-called coupled perturbed Hartree-Fock formalism. Subsequently the sum over excited state formalisms were implemented with the so-called random phase approximation by Lazzeretti and Zanasi and coworkers [50,51]. Finally the first implementation of the tensors, the derivatives of which are required for ROA were first also implemented in CADPAC [52]. Subsequently all of these tensors have now been implemented in the programs Gaussian and Dalton, and in this special issue of TCA the first implementation of the AAT required for VCD with Slater type orbitals is presented, as implemented in the ADF code [53].

4 Conclusions

In this study we have shown that VA and VCD spectroscopy can be used to gain both configurational and conformational information for chiral molecules with flexible side chains. The induced VCD signal from the normal modes localized in normally achiral dial chromophore can be used to give conformational information, and hence the relative orientation of the two aldehyde groups. We have also investigated

the VCD spectra of aframodial and its seven diasteriomers and have shown that the normal modes at lower frequencies can be used to assign the absolute configuration of the diasteriomers. This is important in this molecule since there are four chiral centers and hence eight sets of enantiomers.

Similar to the work on L-histidine in this special issue by Deplazes et al. the use of VA spectroscopy can be used to determine conformational information for small flexible molecules [54], but is supplemented by VCD (and also Raman and ROA) measurements and spectral simulations.

The first measurements of vibrational/infrared circular dichroism in crystals [55] and in solution [56–60] occurred approximately 30 years also. Shortly thereafter, the first VCD measurements were carried out on matrix isolated species [61]. The first ROA measurements were more difficult to obtain, with the first reported results [62], later refuted by L.D. Barron et al. [63]. Initially VCD was limited to ad hoc theories, like the fixed partial charge approximation [64,65], which really limited the application of VCD to take off. It was realized very early that the electronic contribution to the atomic axial tensors was zero within the Born–Oppenheimer approximation [65,66], though the tensors at the time were not yet called the atomic axial tensors. It took approximately 10 years for a rigorous theory of VCD to be developed which could be implemented [67–69], albeit beyond the so-called Born-Oppenheimer approximation. An earlier sum over excited states form was deemed not feasible at the time [70], which was in theory equivalent to the contracted forms of Stephens and Galwas [45,47,67–69]. On the other hand, the theory of ROA was developed before the first measurements [63,71,72]. In the intervening years the theory of VCD which was originally implemented with the so-called common origin (CO) gauge, has been extended to the so-called distributed origin (DO) gauge, which was the first formalism which solved the gauge problem the original formalism [45,47,67–69,73]. Subsequently the gauge problems was addressed with the so-called GIAO method [74–76] and the LORG method [77]. Chiral vibrational spectroscopy which started off as a relatively specialized and esoteric area of research over 30 years ago has come full circle and is now one of the most exciting and intensive areas of research.

By combining and utilizing the latest developments in the chemical, physical, mathematical and electronic research areas research VA/VCD and Raman/ROA spectrometers are now commercially available [78]. In addition, with the development of DFT based methods, one can now calculate the VA, VCD, Raman and ROA spectra of molecules almost quantitatively. This has also been shown by the papers presented in this special issue by Prof. Stephens group [79], the ADF team [53], and Fristrup from the Green Chemistry Group in Copenhagen [80]. What has been more challenging is both the experimental and theoretical simulation of the VA, VCD, Raman and ROA spectra of biomolecules in aqueous environment. There are three nice works by leading groups in this field in this special issue, one on L-histidine by Deplazes et al. [54], one one L-alanine and *N*-acetyl L-alanine *N′*-methylamide by Jalkanen et al. [12] and finally on one helix formation in peptides by the Keiderling group [81].

Finally to be able to assign the bands in the vibrational spectra one requires in addition to the calculated vibrational frequencies and VA, VCD, Raman and ROA intensities, a characterization of the normal modes. The group of Hug has developed a new method which has also been presented for the first time in this special issue [82]. And finally Prof. Nafie has presented a new near resonance theory for Raman and ROA spectral simulations [83].

Experimentally, one is contemplating multidimensional VCD and ROA measurements, similar to the corresponding multidimensional NMR and optical experiments. In this area also a rigorous theoretical understanding will be required to fully understand and utilize the results of the experiments. Never has there been a better time for experimental and theoretical chemists, biophysicists and mathematical biologists to work together. The understanding of life and life processes requires a concerted effort by scientists in many disciplines and subdisciplines. Chiral vibrational spectroscopy is slowly becoming a tool for researchers in the fields of molecular biology, physical biology and biophysics. But here the effects due to the environment are large, and, in addition, temperature effects are vital, as biological process occur at room temperature, where entropic contributions can be large.

Acknowledgments KJJ would like to thank the Danish National Research Foundation (DG) for financial support for his position and computational facilities at the Quantum Protein (QuP) Centre at the Technical University of Denmark in Kgs. Lyngby (2001-2005). KJJ and JDG would like to thank the Western Australian government's Premier Fellowship program for financial support; the iVEC (The hub of advanced computing in Western Australia) and APAC (Australian Partnership for Advanced Computing) for providing computer facilities. SS and MKM would like to thank the Human Frontier Science Program Organization for support (grant no. RG0229/2000-M). RMN, IMD and KJJ would like to thank the Academy of Finland (Center of Excellence Grant 2006-2011).

References

1. Kimbu SF, Njimi TK, Sondengam BL, Akinniyi JA, Connolly JD (1979) J Chem Soc Perkin Trans I, pp 1303–1304
2. Marlier M, Le Guellec G, Lognay G, Wathelet JP, Severin M (1993) Planta Med 59:455
3. Nyasse B, Lenta-Ndjakou B (2000) Pharmazie 55:703
4. Duker-Eshun G, Jaroszewski JW, Asomaning WA, Oppong-Boachie F, Olsen CE, Christensen SB (2002) Planta Med 68:642
5. Tanabe M, Chen Y-D, Saito K, Kano Y (1993) Chem Pharmaceutial Bull 41:710
6. Klyne W, Buckingham J (1978) Atlas of Stereochemistry, 2nd edn. vol 1. Chapman & Hall, London
7. Barltrop JA, Bigley DB (1959) Chem Ind London, pp 1378–1379

8. Jalkanen KJ, Bohr HG, Suhai S (1997) In: Proceedings of the international symposium on theoretical and computational genome research. Suhai S (ed) Plenum Press, New York, pp 255–277
9. Tajkhorshid E, Jalkanen KJ, Suhai S (1998) J Phys Chem B 102:5899
10. Frimand K, Jalkanen KJ, Bohr HG, Suhai S (2000) Chem Phys 255:165
11. Jalkanen KJ, Nieminen RM, Frimand K, Bohr J, Bohr H, Wade RC, Tajkhorshid E, Suhai S (2001) Chem Phys 265:125
12. Jalkanen KJ, Degtyarenko IM, Nieminen RM, Cao X, Nafie LA, Zhu F, Barron LD (2007) Theor Chem Acc doi:10.1007/s00214-007-0361-z
13. Jalkanen KJ, Suhai S (1996) Chem Phys 208 (1996)
14. Deng Z, Polavarapu PL, Ford SJ, Hecht L, Barron LD, Ewig CS, Jalkanen KJ (1996) J Phys Chem 100:2025
15. Han W-G, Jalkanen KJ, Elstner M, Suhai S (1998) J Phys Chem B 102:2587
16. Bohr HG, Jalkanen KJ, Frimand K, Elstner M, Suhai S (1999) Chem Phys 246:13
17. Knapp-Mohammady M, Jalkanen KJ, Nardi F, Wade RC, Suhai S (1999) Chem Phys 240:63
18. Jalkanen KJ, Nieminen RM, Knapp-Mohammady M, Suhai S (2003) Int J Quantum Chem 92:239
19. Bunte SW, Jensen GM, McNesby KL, Goodin DB, Chabalowski CF, Nieminen RM, Suhai S, Jalkanen KJ (2001) Chem Phys 265:13
20. Jürgensen VW, Jalkanen KJ (2006) Phys Biol 3:S63
21. Jalkanen KJ, Jürgensen VW, Degtyarenko IM (2005) Adv Quantum Chemistry 50:91
22. Jalkanen KJ (2003) J Phys Condens, Matter 15:S1823
23. Poon C-D, Samulski ET, Weise CF, Weisshaar JC (2000) J Am Chem Soc 122:5642
24. Weise CF, Weisshaar JC (2003) J Phys Chem B 107:3265
25. Kongsted J, Osted A, Mikkelsen KV, Christiansen O (2002) Chem Phys Lett 364:379
26. Gibson DA, Ionova IV, Carter EA (1995) Chem Phys Lett 240:261
27. Pakoulev A, Wang Z, Pang Y, Dlott DD (2003) Chem Phys Lett 380:404
28. Chestnut DB (2003) Chem Phys Lett 380:251
29. Elstner M, Hobza P, Suhai S, Kaxiras E (2001) J Chem Phys 114:5149
30. Hamm P, Woutersen S, Rueping M (2002) Helvetica Chemica Acta 85:3883
31. Woutersen S, Mu Y, Stock G, Hamm P (2001) PNAS 98:11254
32. Woutersen S, Hamm P (2000) J Phys Chem B 104:11316
33. Morita H, Itokawa H (1986) Chem Lett, pp 1205–1208
34. Itokawa H, Morita M, Mihashi S (1980) Chem Pharm Bull 28:3452
35. Morita H, Itokawa H (1988) Planta Med 54:117
36. Ngo KS, Brown GD (1998) Phytochemistry 47:1117
37. Kimbu SF, Njimi TK, Sondengam BL, Akinniyi JA, Connolly JD (1979) J Chem Soc, Perkin Trans I
38. Ayafor JF, Tchuedem MHK, Nyasse B, Tillequin F, Anke H (1994) Pure Appl Chem 66:2327
39. Morita H, Itokawa H (1988) Plant Med 54:117
40. MacMillan J, Beale MH (1999) Diterpene biosynthesis, (Amsterdam Elsevier), Chap, Isoprenoids including carotenoids and steroids pp 217–243
41. Frisch Æ, Dennington III RD, Keith TA, Millam J, Nielsen AB, Holder AJ, Hiscocks J (1998) GaussView 2.0 Visualization Program, Gaussian, Inc., Wallingford
42. Devlin FJ, Stephens PJ (1987) Applied Spectroscopy 41:1142
43. Jalkanen KJ, Gale JD, Jalkanen GJ, McIntosh DF, El-Azhary AA, Jensen GM (2007) Theor Chem Acc. doi:10.1007/s00214-007-0391-6
44. Amos RD (1987) Ab initio methods in quantum chemistry, Chap. Molecular property derivatives. Wiley, New York, pp 99–153
45. Amos RD, Handy NC, Jalkanen KJ, Stephens PJ (1987) Chem Phys Lett 133:21
46. Amos RD (1984) Chem Phys Lett 108:185
47. Amos RD, Jalkanen KJ, Stephens PJ (1988) J Phys Chem 92:5571
48. Mead CA, Moscowitz A (1967) Int J Quantum Chem 1:243
49. Amos RD (1986) Chem Phys Lett 124:376
50. Jalkanen KJ, Stephens PJ, Lazzeretti P, Zanasi R (1988) J Chem Phys 90:3204
51. Stephens PJ, Jalkanen KJ, Amos RD, Lazzeretti P, Zanasi R (1990) J Phys Chem 94:1811
52. Amos RD (1982) Chem Phys Lett 87:23
53. Nicu VP, Neugebauer J, Wolff SK, Baerends EJ (2007) Theor Chem Acc doi:10.1007/s00214-006-0234-x
54. Deplazes E, van Bronswijk B, Zhu F, Barron LD, Ma S, Nafie LA, Jalkanen KJ (2007) Theor Chem Acc doi:10.1007/s00214-007-0276-8
55. Hsu EC, Holzwarth G (1973) J Chem Phys 59:4678
56. Nafie LA, Cheng JC, Stephens PJ (1975) J Am Chem Soc 97:3842
57. Cheng JC, Nafie LA, Stephens PJ (1975) J Opt Soc Am 65:1031
58. Nafie LA, Keiderling TA, Stephens PJ (1976) J Am Chem Soc 98:2715
59. Holzwarth G, Hsu EC, Mosher HS, Faulkner TR, Moscowitz A (1974) J Am Chem Soc 96:251
60. Keideling TA, Nafie LA (1976) Chem Phys Lett 41:46
61. Schlosser DW, Devlin F, Jalkanen K, Stephens PJ (1982) Chem Phys Lett 88:286
62. Bosnich B, Moscowitz, Ozin G (1972) J Am Chem Soc 94:4750
63. Barron LD, Bogaard MP, Buckingham AD (1973) J Am Chem Soc 95:603
64. Schellman JA (1973) J Chem Phys 58:2882
65. Stephens PJ, Jalkanen KJ, Kawiecki RW (1990) J Am Chem Soc 112:6518
66. Cohan NV, Hameka HF (1966) J Am Chem Soc 88:2136
67. Stephens PJ (1985) J Phys Chem 89:748
68. Stephens PJ (1987) J Phys Chem 91:1712
69. Buckingham AD, Fowler PW, Galwas PA (1987) Chem Phys 112:1
70. Craig DP, Thirunamachandran T (1978) Mol Phys 35:825
71. Barron LD, Buckingham AD (1971) Mol Phys 20:1111
72. Buckingham AD (1967) Adv Chem Phys 12:107
73. Jalkanen KJ, Stephens PJ, Amos RD, Handy NC (1988) J Phys Chem 92:1781
74. Bak KL, Jørgensen P, Helgaker T, Ruud K, Jensen HJAa (1993) J Chem Phys 98:8873
75. Bak KL, Jørgensen P, Helgaker T, Ruud K, Jensen HJAa (1994) J Chem Phys 100:6621
76. Bak KL, Devlin FJ, Ashvar CS, Taylor PR, Frisch MJ, Stephens PJ (1995) J Phys Chem 99:14918
77. Hansen AE, Stephens PJ, Bouman TD (1991) J Phys Chem 95: 4255
78. Cao X, Dukor RK, Nafie LA (2007) Theor Chem Acc doi:10.1007/s00214-007-0284-8
79. Stephens PJ, Devlin FJ, Schürch S, Hulliger J (2007) Theor Chem Acc doi:10.1007/s00214-006-0245-7
80. Fristrup P, Lassen PR, Tanner D, Jalkanen KJ (2007) Theor Chem Acc doi:10.1007/s00214-006-0186-1
81. Kim J, Kapitan J, Lakhani A, Bour P, Keiderling TA (2007) Theor Chem Acc doi:10.1007/s00214-006-0183-4
82. Hug W, Fedorovsky M (2006) Theor Chem Acc doi:10.1007/s00214-006-0185-2
83. Nafie LA (2007) Theor Chem Acc doi:10.1007/s00214-007-0267-9